Two-body strong decays of the 2*P* and 3*P* charmonium states

Zhi-Hui Wang[1,2,3,*] and Guo-Li Wang[4,5,†]

[1]*Key Laboratory of Physics and Photoelectric Information Functional Materials, North Minzu University, Yinchuan 750021, China*
[2]*School of Electrical and Information Engineering, North Minzu University, Yinchuan 750021, China*
[3]*School of Physics and Center of High Energy Physics, Peking University, Beijing 100871, China*
[4]*Department of Physics, Hebei University, Baoding 071002, China*
[5]*Hebei Key Laboratory of High-precision Computation and Application of Quantum Field Theory, Baoding 071002, China*

Two-body open charm strong decays of the 2*P* and 3*P* charmonium states are studied by the Bethe-Salpeter method combined with the $^3P_0$ model. The wave functions and mass spectra of the 2*P* and 3*P* charmonium states are obtained by solving the Bethe-Salpeter equation with the relativistic correction. The strong decay widths and relative ratios of the 2*P* and 3*P* charmonium states are calculated. Comparing our results with the experimental data, we obtain some interesting results. Considering the $X^*(3860)$ as the $\chi_{c0}(2P)$, the total strong decay width is smaller than the experimental data. But the strong decay width depends on the parameter γ in the $^3P_0$ model, and the mass and width of the $X^*(3860)$ have large errors, we cannot rule out the possibility that the $X^*(3860)$ is the $\chi_{c0}(2P)$. The $X(4160)$ is a good candidate for the $\chi_{c0}(3P)$, not only the strong decay width of the $\chi_{c0}(3P)$ is same as the experimental data, but the relative ratios $\frac{\Gamma(\chi_{c0}(3P)\to D\bar{D})}{\Gamma(\chi_{c0}(3P)\to D^*\bar{D}^*)} \approx 0.0019 < 0.09$, and $\frac{\Gamma(\chi_{c0}(3P)\to D\bar{D}^*)}{\Gamma(\chi_{c0}(3P)\to D^*\bar{D}^*)} = 0 < 0.22$ are consistent with the experimental results of the $X(4160)$. Taking the $X(4274)$ as the $\chi_{c1}(3P)$, the strong decay width is consistent with the experimental data, so the $X(4274)$ is a good candidate for the $\chi_{c1}(3P)$. Assigning the $X(4350)$ as the $\chi_{c2}(3P)$, the corresponding strong decay width is slightly larger than the experimental data. To identify if the $X(4350)$ is $\chi_{c2}(3P)$, many more investigations are needed. All of the strong decay widths and relative ratios of the 2*P* and 3*P* charmonium states can provide the useful information to discover and confirm these particles in the future.

I. INTRODUCTION

Since the Belle Collaboration reported the first observation of the $X(3872)$ [1], many more charmoniumlike states have been observed experimentally. Belle observed the $X(4160)$ from the process $e^+e^- \to J/\psi D^*\bar{D}^*$, which has the mass and width $M = (4156^{+25}_{-20} \pm 15)$ MeV and $\Gamma = (139^{+111}_{-61} \pm 21)$ MeV, respectively [2]. They also gave the upper limits of relative ratios: $\frac{B_{D\bar{D}}(X(4160))}{B_{D^*\bar{D}^*}(X(4160))} < 0.09$, $\frac{B_{D^*\bar{D}}(X(4160))}{B_{D^*\bar{D}^*}(X(4160))} < 0.22$. The $X(4140)$ was first observed by the CDF Collaboration in the exclusive decay $B \to J/\psi\phi K$ [3], then another charmoniumlike states the $X(4274)$

also was observed in the same decay channel [4]. These two charmoniumlike states also were observed by LHCb Collaboration [5,6], the mass and natural width of $X(4140)$ and $X(4274)$ were $M = (4146.8 \pm 2.4)$ MeV, $\Gamma = (22^{+8}_{-7})$ MeV, and $M = (4274^{+8}_{-6})$ MeV, $\Gamma = (49 \pm 12)$ MeV [7], respectively. In 2010, *BABAR* observed the $Z(3930)$ in the $\gamma\gamma$ production of $D\bar{D}$ system [8]. Now the Particle Data Group gives the mass and width of the $Z(3930)$ as $M = (3927.2 \pm 2.6)$ MeV and $\Gamma = (24 \pm 6)$ MeV [7]. And the properties of $Z(3930)$ are consistent with the expectations for the $\chi_{c2}(2P)$ state [9,10]. Belle also explored a charmoniumlike state $X(4350)$ in the process $J/\psi\phi$ in 2010, the extracted mass and width were $(4350.6^{+4.6}_{-5.1})$ and $(13^{+18}_{-9} \pm 4)$ MeV [11]. The $X^*(3860)$ was observed in the process $e^+e^- \to J/\psi D\bar{D}$ by Belle in 2017, the corresponding mass and width are $M = (3862^{+26+40}_{-32-13})$ MeV and $\Gamma = (201^{+154+88}_{-67-82})$ MeV [12], respectively.

The properties of these charmoniumlike states have inspired great interest in both theoretical and experimental research fields of hadronic physics. Many theoretical

[*]zhwang@nmu.edu.cn
[†]wgl@hbu.edu.cn

approaches have studied the properties of these charmoniumlike states [13–28]. Reference [15] investigated that the $X(4140)$ and $X(4274)$ can be both interpreted as the S-wave $cs\bar{c}\bar{s}$ tetraquark states of $J^P = 1^+$. Reference [16] computed the open-charm strong decay widths of the $\chi_c(3P)$ states and their radiative transitions, and they suggested the $X(4274)$ could be interpreted as the $\chi_{c1}(3P)$ state. Taking the $Z(3930)$ as $\chi'_{c2}(2P)$, the Ref. [19] investigated the decay $Z(3930)$ into $J/\psi\omega$. Considering the $X(4350)$ as the χ''_{c2}, the Ref. [23] analyzed the mass and calculated the open charm strong decay of the $X(4350)$, which were consistent with the existing experimental data. The results of Ref. [25] preferred the $J^{PC} = 0^{++}$ assignment for the $X^*(3860)$ over the 2^{++} assignment, which was also in agreement with the experiment. Calculating the observable quantity (such as the spectrum or the strong decay width) of these charmoniumlike states, then comparing with the experimental data, may help us to better understand the quark structure of the charmoniumlike states.

In addition to the mass spectrum and strong decay width, the electromagnetic decay also can help us to determine the structure these charmonium-like states. According to E1 transition widths for the $\chi_{c1}(2P) \rightarrow \gamma J/\psi$ and $\chi_{c1}(2P) \rightarrow \gamma\psi(2S)$ and other results, the Ref. [29] argued that the $X(3872)$ may be a $\chi_{c1}(2P)$ dominated charmonium state with some admixture of the $D^0\bar{D}^{*0}$ component. The Ref. [30] calculated the one- and two-photon decay widths of $Y(3940)$, $Z(3930)$, $X(3915)$, and $X(4160)$ mesons. Considering $X(4660)$, $X(3872)$, $X(3900)$, $X(3915)$, and $X(4274)$ as 5^3S_1, 2^3P_1, 2^1P_1, 2^3P_0, and 3^3P_1, respectively, the Ref. [31] studied the E1 and M1 transition width, and annihilation decays of these charmonium states. But the electromagnetic decay widths of these charmonium states are about the order of keV, which are smaller than the results of Okubo-Zweig-Iizuka (OZI)-allowed strong decay. These electromagnetic decays can only be detected experimentally when large amounts of data are available in the future. For now, the strong decay widths and the relative ratios of these charmonium states are good ways to determine their properties.

In this paper we will focus on the strong decay widths of the $2P$ and $3P$ charmonium states. The relativistic correction of the $2P$ and $3P$ charmonium states are larger than that of the corresponding $1P$ states, therefore, we need a relativistic model. The Bethe-Salpeter (BS) method is a relativistic framework that describes the bound state with definite quantum number, the corresponding relativistic form of wave functions are the solutions of the full Salpeter equations. Using the BS method, we have discussed the properties of some radial excited states in previous work, such as the semileptonic and nonleptonic B_c decays to the $Z(3930)$ and $X(4160)$ as the $\chi_{c2}(2P)$ and $\chi_{c2}(3P)$ [32], the strong decays of the $X(3940)$ and $X(4160)$ as radial high excited states the $\eta_c(3S)$ and $\eta_c(4S)$ [33], the radiative E1 decay of the $X(3872)$ [34,35], two-body strong decay of

the $Z(3930)$ which was the $\chi_{c2}(2P)$ state [36]. All the theoretical results are consistent with the experimental data or other theoretical results. So the BS method is a good way to describe the properties and decays of the radially higher excited states. In this paper, we will study the strong decays of the $2P$ and $3P$ charmonium states by the BS method with the $^3P_0$ model.

For the $2P$ and $3P$ charmonium states, the dominant decay is the OZI-allowed two-body open charm strong decay. We will adopt the $^3P_0$ model to calculate the two-body open charm strong decay. The $^3P_0$ model was used to calculate the decay rates of the meson resonances in Ref. [37], which assumed that the $q\bar{q}$ pair is produced from vacuum with quantum number $J^{PC} = 0^{++}(^3P_0)$, was applied to calculate the strong decay of heavy-light mesons [23,38] and heavy quarkonia [26,39]. We also studied the strong decays of some heavy quarkonia by the $^3P_0$ model combine with the BS method in Refs. [33,36,40], the results were in accordance with the experimental data or other theoretical results. So we take the same model to calculate the two-body open charm decay of the $2P$ and $3P$ charmonium states.

The paper is organized as follows. We give the formulation of two-body strong decay of charmonium state in Sec. II. In Sec. III, we show the numerical results and discussions. We give the corresponding conclusions in Sec. IV. Finally, we present the instantaneous BS equation and the relativistic wave functions of P-wave charmonium states in the Appendices.

II. TWO-BODY STRONG DECAY OF CHARMONIUM STATE

To calculate the two-body open charm strong decays of the $2P$ and $3P$ charmonium states by the relativistic BS method, we extend the $^3P_0$ model to relativistic form: $H = -ig \int d^4x\bar{\psi}\psi$ [36,40]. Here ψ is the dirac quark field, $g = 2\gamma m_q$, m_q is the quark mass of the light quark-pairs, γ is a dimensionless constant that describes the pair-production strength. In this paper, we take $\gamma = 0.35$, which is the best-fit value for the usual $^3P_0$ model [28]. Combining the $^3P_0$ model with the BS wave functions of the initial and final mesons, the corresponding amplitude in Fig. 1 can be written as
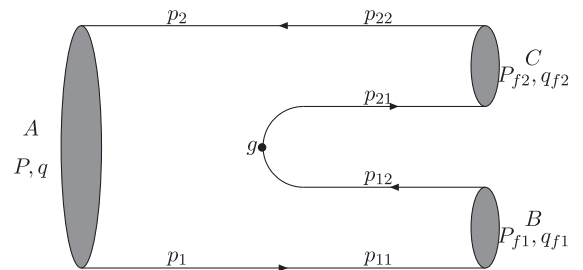

FIG. 1. The Feynman diagram of two-body open charm strong decay.

$$\mathcal{M} = \langle BC|H|A\rangle = -ig \int \frac{\mathrm{d}^4 q}{(2\pi)^4} \mathrm{Tr}[\chi_P(q)S_2^{-1}(p_2)\bar{\chi}_{P_{f2}}(q_{f2})\bar{\chi}_{P_{f1}}(q_{f1})S_1^{-1}(p_1)]. \tag{1}$$

Integrating out the momentum q_0 with instantaneous approximation, and neglecting all the negative energy contributions which have very small influence on the amplitude [40], then the leading order amplitude Eq. (1) is the overlap integration of the positive BS wave functions for the initial and final states,

$$\mathcal{M} = \langle BC|H|A\rangle = g \int \frac{\mathrm{d}^3\vec{q}}{(2\pi)^3} \mathrm{Tr}\left[\frac{\not{P}}{M}\varphi_P^{++}(\vec{q})\frac{\not{P}}{M}\bar{\varphi}_{P_{f2}}^{++}(\vec{q}_{f2})\bar{\varphi}_{P_{f1}}^{++}(\vec{q}_{f1})\right]\left(1 - \frac{M - \omega_1 - \omega_2}{2\omega_{12}}\right), \tag{2}$$

where $\varphi_P^{++}(\vec{q})$, $\varphi_{P_{f1}}^{++}(\vec{q}_{f1})$, and $\varphi_{P_{f2}}^{++}(\vec{q}_{f2})$ are the positive BS wave functions of the initial meson A, finial meson B and C, respectively. $\bar{\varphi} = \gamma^0\varphi^\dagger\gamma^0$. $\vec{q}$, $\vec{q}_{f1}$, $\vec{q}_{f2}$ are the three dimensions relative momentum between the quark and antiquark of the initial meson A, finial meson B and C, respectively. $\vec{q}_{f1} = \vec{q} - \frac{m_c}{m_c + m_{u,d,s}}\vec{P}_{f1}$, $\vec{q}_{f2} = \vec{q} + \frac{m_c}{m_c + m_{u,d,s}}\vec{P}_{f2}$. $\vec{P}_{f1}$ and $\vec{P}_{f2}$ are the three momentum of finial mesons B and C. $w_{12} = \sqrt{m_{u,d,s}^2 + \vec{q}_{f1}^2}$.

Finally, the two-body open charm strong decay width of the 2P and 3P charmonium states can be expressed as

$$\Gamma = \frac{|\vec{P}_{f1}|}{8\pi M^2(2J+1)}\sum_\lambda |\mathcal{M}|^2, \tag{3}$$

where $|\vec{P}_{f1}| = \sqrt{[M^2 - (M_{f1} - M_{f2})^2][M^2 - (M_{f1} + M_{f2})^2]}/(2M)$, which is the three momentum of the final mesons.

III. NUMERICAL RESULTS AND DISCUSSIONS

In order to fix the parameters in Cornell potential in Eq. (A8) and masses of quarks, we take $a = e = 2.7183$, $\lambda = 0.21$ GeV^2, $\Lambda_{\mathrm{QCD}} = 0.27$ GeV, $\alpha = $

0.06 GeV, $m_c = 1.62$ GeV, $m_u = 0.305$ GeV, $m_d = 0.311$ GeV, $m_s = 0.500$ GeV, etc. [41,42], which give the best to fit the mass spectra of the ground charmonium states and other heavy meson states. The corresponding mass spectra of the P-wave charmonium states are shown in Table I which are obtained by solving the coupled Salpeter equations Eq. (A7).

A. $\chi_{c0}(2P)$ and $\chi_{c0}(3P)$

First, we study the higher charmonium states with $J^{PC} = 0^{++}$, $\chi_{c0}(2P)$ and $\chi_{c0}(3P)$, and give the two-body open charm strong decay results in Table II. The mass $M_{\chi_{c0}(2P)} = 3836.8$ MeV is close to the result of the screened potential model (3842 MeV) [29] and the non-relativistic potential model (3852 MeV) [26]. Limited by phase space, there is one decay mode $0^{++} \to 0^-0^-$ for the $\chi_{c0}(2P)$, the corresponding decay channel only includes $D\bar{D}$ within the kinematic ranges. And we also get the total strong decay widths of the $\chi_{c0}(2P)$: $\Gamma = 21.0$ MeV, which is in accordance with the result of the linear potential quark model (22 MeV) [24] and the usual $^3P_0$ model (23 MeV) [28].

Belle reported a charmonium-like state $X^*(3860)$, and they claimed that the $X^*(3860)$ seems to be a candidate of

TABLE I. The Mass spectra of P-wave charmonia (unit in MeV) [42]. The experimental data from the Particle Data Group [7].

$(n^{2S+1}L_J)J^{PC}$	Our results	Screened potential model [29]	Godfrey-Isgur nonrelativistic model [26]	Experimental data from the Particle Data Group
$(1^3P_0)0^{++}$	3414.7(input)	3433	3445(3424)	3414.71 ± 0.30
$(2^3P_0)0^{++}$	3836.8	3842	3916(3852)	$\cdots$
$(3^3P_0)0^{++}$	4140.1	4131	4292(4202)	$\cdots$
$(1^3P_1)1^{++}$	3510.3(input)	3510	3510(3505)	3510.67 ± 0.05
$(2^3P_1)1^{++}$	3928.7	3901	3953(3925)	$\cdots$
$(3^3P_1)1^{++}$	4228.8	4178	4317(4271)	$\cdots$
$(1^3P_2)2^{++}$	3556.1(input)	3554	3550(3556)	3556.17 ± 0.07
$(2^3P_2)2^{++}$	3972.4	3937	3979(3972)	$\cdots$
$(3^3P_2)2^{++}$	4271.0	4208	4337(4317)	$\cdots$
$(1^1P_1)1^{+-}$	3526.0(input)	3519	3517(3516)	3525.38 ± 0.11
$(2^1P_1)1^{+-}$	3943.0	3908	3956(3934)	$\cdots$
$(3^1P_1)1^{+-}$	4242.4	4184	4318(4279)	

TABLE II.   The strong decay type and decay widths of the $\chi_{c0}(2P)$ and $\chi_{c0}(3P)$ (unit in MeV). The results in the parentheses are calculated with $M_{\chi_{c0}(2P)} = 3862.0$ MeV and $M_{\chi_{c0}(3P)} = 4156.0$ MeV.

Meson	State	Mode	Our result	LP(SP) [24]	[26]	[27]	[28]
χ_{c0}	2^3P_0	$D\bar{D}$	21.0(16.4)	22(28)	30	$\cdots$	23
	3^3P_0	$D\bar{D}$	0.17(0.13)	0.04(0.08)	0.5	2	$\cdots$
		$D^*\bar{D}^*$	79.0(69.4)	21(30)	43	67	$\cdots$
		D_sD_s	1.7(1.8)	8.9(9)	6.8	3	$\cdots$
		$D_s^*D_s^*$	$\cdots$	2.7(–)	$\cdots$	$\cdots$	$\cdots$
		Total	81(71)	33(39)	51	72	$\cdots$

the $\chi_{c0}(2P)$ state [12]. Reference [24] studied the strong decays of the $X^*(3860)$ as $\chi_{c0}(2P)$ by linear potential (LP) and screened potential (SP) models, and they gave a similar value $\Gamma \approx 22$–28 MeV. The analysis of Ref. [43] showed that the $X^*(3860)$ was an indication of the $\chi_{c0}(2P)$ state. Assuming the $X^*(3860)$ as the $\chi_{c0}(2P)$, the Ref. [44] calculated the strong decay of the $\chi_{c0}(2P)$, the total decay of the $X^*(3860)$ state ranged from 110 to 180 MeV with $R = 2.3$–2.5 GeV^{-1}, the corresponding decay mode and total decay width were consistent with the experimental data. Taking the $X^*(3860)$ as the $\chi_{c0}(2P)$, we get the strong decay width $\Gamma = 16.4$ MeV, which is smaller than the center value of the $X^*(3860)$: $(201^{+154+88}_{-67-82})$ MeV. But the strong decay width is related to the parameter γ in the $^3P_0$ model, the result increases with the parameter γ. In addition, considering the large uncertainties of the mass and decay width for the $X^*(3860)$, we cannot exclude that the $X^*(3860)$ is $\chi_{c0}(2P)$. And more investigations are needed to confirm the property of the $X^*(3860)$ in the future.

By solving the Eq. (A7), we get the mass of $\chi_{c0}(3P)$ as: $M_{\chi_{c0}(3P)} = 4140.1$ MeV, which is close to the result of the screened potential model (4131 MeV) [29]. The dominant strong decay of the is OZI-allowed two-body open charm strong decay. And there are two decay types: $0^{++} \rightarrow 0^-0^-$ and $0^{++} \rightarrow 1^-1^-$, while the decay mode $0^{++} \rightarrow 0^-1^-$ is forbidden. Therefore, the final mesons include $D\bar{D}$, D_sD_s, and $D^*\bar{D}^*$ within the kinematic ranges, and there is no $D\bar{D}^*$. The decay channel $\chi_{c0}(3P) \rightarrow D\bar{D}$ has the largest phase space, but due to the node structure of $\chi_{c0}(3P)$'s wave functions, the integrand (which consists of the overlapped wave functions) oscillates accordingly in the amplitude. The positive contribution of the integrand almost cancels the negative contribution in $\chi_{c0}(3P) \rightarrow D\bar{D}$, leading to a smallest value of $\chi_{c0}(3P) \rightarrow D\bar{D}$ in Table II. So the dominant contribution comes from $\chi_{c0}(3P) \rightarrow D^*\bar{D}^*$, which is consistent with the result of the screened potential model [29]. Then we calculate all of the two-body open charm strong decays, the total strong decay width $\Gamma_{\chi_{c0}(3P)} = 81$ MeV is close to the result of the unquenched quark model (71 MeV) [27].

The $X(4160)$ was observed by Belle from the process $e^+e^- \rightarrow J/\psi D^*\bar{D}^*$ [2]. References [29,45] discussed

possible interpretations for the $X(4160)$ based on the Nonrelativistic quantum chromodynamics calculations and the potential model, two likely assignments for the $X(4160)$ were $\chi_{c0}(3P)$ and $\eta_c(4S)$. Reference [46] calculated the strong decays of the $\eta_c(nS)$, and they found both that the explanation of the $X(3940)$ as $\eta_c(3S)$ is possible and that the assignment of the $X(4160)$ as $\eta_c(4S)$ cannot be excluded. Reference [47] calculated the strong decay of the $X(4160)$, which was assumed as the $\chi_{c0}(3P)$, $\chi_{c1}(3P)$, $\eta_{c2}(2D)$, or $\eta_c(4S)$ by the $^3P_0$ model, they thought that the excited charmonium state $\eta_c(4S)$ cannot be ruled out as an assignment for the $X(4160)$. Considering the $X(4160)$ as the $\eta_c(4S)$ state, we also calculated the strong decay of the $\eta_c(4S)$ in Ref. [33], the ratio of the decay width $\frac{\Gamma(D\bar{D}^*)}{\Gamma(D^*\bar{D}^*)}$ of $\eta_c(4S)$ was larger than the experimental data of the $X(4160)$, thus, the $X(4160)$ was not the candidate of the $\eta_c(4S)$. In this work, the mass of $\chi_{c0}(3P)$ is close to the $X(4160)$, assigning the $X(4160)$ as the $\chi_{c0}(3P)$, the total strong decay width $\Gamma_{\chi_{c0}(3P)} = 71$ MeV is rough consistent with the result of experimental results for $X(4160)$: $(139^{+111}_{-61} \pm 21)$ MeV. Then we calculate relative ratios $\frac{\Gamma(\chi_{c0}(3P) \rightarrow D\bar{D})}{\Gamma(\chi_{c0}(3P) \rightarrow D^*\bar{D}^*)} \approx 0.0019 < 0.09$, and $\frac{\Gamma(\chi_{c0}(3P) \rightarrow D\bar{D}^*)}{\Gamma(\chi_{c0}(3P) \rightarrow D^*\bar{D}^*)} = 0 < 0.22$, both of which agree with the experimental results of $X(4160)$ by the Belle Collaboration [2]. Therefore, $X(4160)$ is a good candidate for $\chi_{c0}(3P)$.

B. $\chi_{c1}(2P)$ and $\chi_{c1}(3P)$

Using the BS method, we get the masses and wave functions of the $\chi_{c1}(2P)$ and $\chi_{c1}(3P)$. The $M_{\chi_{c1}(2P)} = 3928.7$ MeV is close to the result of the nonrelativistic potential model (3925 MeV) [26]. The two-body open charm strong decay results have been shown in Table III. For the $\chi_{c1}(2P)$, there is only one decay mode $1^{++} \rightarrow 0^-1^-$, so the final state include DD^* state. The corresponding decay width $\Gamma_{\chi_{c1}(2P)} = 103$ MeV is the same as the results of linear potential quark model (102 MeV) [24], but smaller than the results of other methods.

The mass $M_{\chi_{c1}(3P)} = 4228.8$ MeV is larger than the result of the screened potential model (4178 MeV) [29], but smaller the than results of the relativized Godfrey-Isgur model (4317 MeV) and nonrelativistic potential model

TABLE III.   The strong decay type and decay widths of the $\chi_{c1}(2P)$ and $\chi_{c1}(3P)$ (unit in MeV). The results in the parentheses are calculated with $M_{\chi_{c1}(3P)} = 4274.0$ MeV.

Meson	State	Mode	Our result	[16]	LP(SP) [24]	[26]	[27]	[28]
χ_{c1}	2^3P_1	DD^*	103	$\cdots$	102(127)	165	$\cdots$	127
	3^3P_1	DD^*	14.3(24.9)	6.6	7.1(5.3)	6.8	20	$\cdots$
		$D^*\bar{D}^*$	9.0(14.7)	28	0.2(1.1)	19	26	$\cdots$
		$D_s D_s^*$	6.0(10.2)	6.3	11(8.0)	9.7	$\cdots$	$\cdots$
		$D_s^* D_s^*$	0.4(2.9)	2.5	5.5(–)	2.7	2	$\cdots$
		DD_0	0.01(0.02)	0.2	0.001(–)	0.1	$\cdots$	$\cdots$
		Total	29.7(52.7)	43.6	23(14)	39	48	$\cdots$

(4271 MeV) [26]. The two-body open charm strong decay of $\chi_{c1}(3P)$ have three decay modes: $1^{++} \to 0^-1^-, 1^-1^-, 0^-0^+$ and include five final states: DD^*, $D^*\bar{D}^*$, $D_s D_s^*$, $D_s^* D_s^*$, DD_0. The dominant strong decay channels are DD^*, $D^*\bar{D}^*$, and $D_s D_s^*$. The ratios between different partial width are independent of the strength parameter γ, they are $\frac{\Gamma(\chi_{c1}(3P) \to D^*\bar{D}^*)}{\Gamma(\chi_{c1}(3P) \to DD^*)} \approx 0.63$ and $\frac{\Gamma(\chi_{c1}(3P) \to D_s D_s^*)}{\Gamma(\chi_{c1}(3P) \to DD^*)} \approx 0.42$, which can be explored in the future experiment. The total strong decay width $\Gamma_{\chi_{c1}(3P)} = 29.7$ MeV, which is similar to the result of the linear potential quark model (23 MeV) and the relativized Godfrey-Isgur model (39 MeV) [26], but smaller than the result of the unquenched quark model (48 MeV) [27].

Some charmoniumlike states with $J^{PC} = 1^{++}$: $X(3872)$, $X(4274)$, have been discovered in experiments [7]. They may be the good candidates for the $\chi_{c1}(nP)$. Reference [48] calculated the E1 radiative and strong decays of the $X(3872)$ as all possible $1D$ and $2P$ $c\bar{c}$ states. The Ref. [49] explored the 1^3D_2, 1^3D_3, and 2^1P_1 charmonium candidates for $X(3872)$, and the 1^3D_2, 1^3D_3 were favored candidates for the $X(3872)$, both have prominent radiative decays. The $X(3872)$ was examined by the molecule model and the charmonium model in Ref. [50], the author thought that the $X(3872)$ may fit more likely to the excited $^3P_1$ charmonium than to the molecule. The quantum number of the $X(3872)$ is the same as $\chi_{c1}(2P)$, but its mass is about 50 MeV lighter than the result of our prediction. Considering the $X(3872)$ as the $\chi_{c1}(2P)$, we have calculated the radiative $E1$ decay widths of the $X(3872)$ through the BS method in Ref. [34], the result was in agreement with the experimental data. However, there is no two-body open charm strong decay for $X(3872)$, which has a narrow width $\Gamma_{X(3872)} < 1.2$ MeV [7]. Because the mass of $X(3872)$ happens to lie around the $D\bar{D}^*$ threshold, many authors believed that it is an ideal candidate for the $D\bar{D}^*$ exotic hadrons. Various scenarios have been discussed in the literature Refs. [51–55], but until now, the nature of the $X(3872)$ still remains unclear, many more investigations are very essential to understand the property of the $X(3872)$ in the future.

Reference [16] calculated the strong decay of $X(4274)$ as $\chi_{c1}(3P)$ with $M = 4317$ MeV, and they got the width

$\Gamma = 43.6$ MeV. Reference [27] gave the decay width of $\chi_{c1}(3P)$: $\Gamma = 48$ MeV, which was consistent with experimental data, and it was possible to assign $X(4274)$ as the $\chi_{c1}(3P)$ state. Considering the $X(4274)$ as the $\chi_{c1}(3P)$ state, we calculate its strong decays by the BS method. The total strong decay width $\Gamma = 52.7$ MeV is larger than 29.7 MeV with $M_{\chi_{c1}(3P)} = 4228.8$ MeV, so the strong decay width is sensitive to the mass of the $\chi_{c1}(3P)$. The total strong decay width $\Gamma = 52.7$ MeV is in agreement with the world average data $\Gamma_{X(4274)} = (49 \pm 12)$ MeV [7]. Therefore, the $X(4274)$ is a good candidate for the $\chi_{c1}(3P)$ state. Assigning the $X(4274)$ as the $\chi_{c1}(3P)$, the relative ratios are $\frac{\Gamma(\chi_{c1}(3P) \to D^*\bar{D}^*)}{\Gamma(\chi_{c1}(3P) \to DD^*)} \approx 0.59$ and $\frac{\Gamma(\chi_{c1}(3P) \to D_s D_s^*)}{\Gamma(\chi_{c1}(3P) \to DD^*)} \approx 0.41$, which can provide more useful information to observe the $X(4274)$ in the future experiment.

C. $\chi_{c2}(2P)$ and $\chi_{c2}(3P)$

By solving the Eq. (A7), we also obtain the mass of $\chi_{c2}(2P)$ and $\chi_{c2}(3P)$, the $M_{\chi_{c2}(2P)} = 3972.4$ MeV is in accordance with the relativized Godfrey-Isgur model (3979 MeV) and the nonrelativistic potential model (3972 MeV) [26]. $M_{\chi_{c2}(3P)} = 4271.0$ MeV is smaller than the mass in the relativized Godfrey-Isgur model (4337 MeV) and the nonrelativistic potential model (4317 MeV) [26]. The two-body open charm strong decays of the $\chi_{c2}(2P)$ and $\chi_{c2}(3P)$, are shown in Table IV. The $\chi_{c2}(2P)$ state has two decay modes: $2^{++} \to 0^-0^-, 0^-1^-$, and the corresponding final states include $D\bar{D}$, DD^*, and $D_s D_s$. We find that the dominant channels are $D\bar{D}$ and DD^*, the $\chi_{c2}(2P) \to D_s D_s$ is very small with the small phase space. Then the total strong decay width $\Gamma_{\chi_{c2}(2P)} = 46$ MeV, which is smaller than the results of the nonrelativistic potential model (80 MeV) [26] and the usual $^3P_0$ model (60.5 MeV) [28].

There are three decay modes for the $\chi_{c2}(3P)$: $2^{++} \to 0^-0^-, 0^-1^-, 1^-1^-$, and six strong decay channels $D\bar{D}$, DD^*, $D^*\bar{D}^*$, $D_s D_s$, $D_s D_s^*$, and $D_s^* D_s^*$. The total strong decay width $\Gamma = 36$ MeV is consistent with the results of linear potential quark model (43 MeV) and screened potential quark model (30 MeV) [24]. $\chi_{c2}(3P) \to D^*\bar{D}^*$ is the dominant decay channel, which contributes about

TABLE IV. The strong decay type and decay widths of the $\chi_{c2}(2P)$ and $\chi_{c2}(3P)$ (unit in MeV). The results in the parenthese are calculated with $M_{\chi_{c2}(2P)} = 3930.0$ MeV and $M_{\chi_{c2}(3P)} = 4350.0$ MeV.

Meson	State	Mode	Our result	LP(SP) [24]	[26]	[27]	[28]
χ_{c2}	2^3P_2	$D\bar{D}$	24.6(20.4)	$\cdots$	42	$\cdots$	32
		DD^*	21.1(6.9)	$\cdots$	37	$\cdots$	28
		D_sD_s	0.6(–)	$\cdots$	0.7	$\cdots$	0.5
		total	46(27.3)	$\cdots$	80	$\cdots$	60.5
	3^3P_2	$D\bar{D}$	5.7(8.7)	8.1(7.3)	8.0	7	$\cdots$
		DD^*	2.2(2.7)	17(13)	2.4	3	$\cdots$
		$D^*\bar{D}^*$	24.3(28.6)	4.2(7.1)	24	39	$\cdots$
		D_sD_s	0.4(0.9)	1.0(0.6)	0.8	0	$\cdots$
		$D_sD_s^*$	3.0(4.2)	0.3(1.4)	11	$\cdots$	$\cdots$
		$D_s^*D_s^*$	0.6(1.8)	4.8(–)	7.2	1	$\cdots$
		DD_1	–(0.9)	1.0(0)	1.1	$\cdots$	$\cdots$
		DD_1'	–(10.9)	7.3(0)	12	$\cdots$	$\cdots$
		DD_2	–(1.4)	$\cdots$	$\cdots$	$\cdots$	$\cdots$
		D^*D_0	–(0.3)	$\cdots$	$\cdots$	$\cdots$	$\cdots$
		Total	36(60)	43(30)	66	50	–

68% of the total strong decay width. We also predict the relative ratios $\frac{\Gamma(\chi_{c2}(3P)\to D\bar{D})}{\Gamma(\chi_{c2}(3P)\to D^*\bar{D}^*)} \approx 0.23$ and $\frac{\Gamma(\chi_{c2}(3P)\to DD^*)}{\Gamma(\chi_{c2}(3P)\to D^*\bar{D}^*)} \approx$ 0.091 with $M_{\chi_{c2}(3P)} = 4271.0$ MeV.

Reference [56] studied the strong decays of the $\chi_{cJ}(2P)$ and $\chi_{cJ}(3P)$, the mass of $\chi_{c2}(2P)$ was very close to the experimental data of the $Z(3930)$, but the decay width $\Gamma \approx 68$ MeV, which was three times that of the experimental value. The $Z(3930)$ was assigned to the $\chi_{c2}(2P)$, and the strong decay width was $\Gamma = 19.0$ MeV in the Ref. [57]. Assigning the $Z(3930)$ as the $\chi_{c2}(2P)$, we have taken two methods to calculate the OZI-allowed two-body strong decay processes of the $\chi_{c2}(2P)$ state in detail: the BS method and the extended $^3P_0$ model in Ref. [36]. The total decay width is consistent with the experimental data, which means that $Z(3930)$ is a good candidate for the $\chi_{c2}(2P)$, so we only list the total strong decay width of the $\chi_{c2}(2P)$ in this paper.

$X(4350)$ was observed by Belle in the $\phi J/\psi$ mass spectrum, which is a candidate for the $\chi_{c2}(3P)$ [11]. The open-charm decay of $\chi_{c2}(3P)$ with $R = 1.9 \approx 2.3$ GeV^{-1} was well consistent with experimental data of the $X(4350)$, which showed that the $X(4350)$ as a good candidate of $\chi_{c2}(3P)$ in Ref. [23]. Assigning the $X(4350)$ as the $\chi_{c2}(3P)$ state, the Ref. [24] studied its the strong decay, and got the decay width which was about 90 MeV. Considering the $X(4350)$ as the $\chi_{c2}(3P)$, some new decay channels are allowed with the increasing mass, such as DD_1, DD_1', DD_2, and D^*D_0. So the total decay width increases to $\Gamma = 60$ MeV, which is consistent with the results of the nonrelativistic potential model (66 MeV) [26], but larger than the result of experimental data $\Gamma_{X(4350)} = (13^{+18}_{-9} \pm 4)$ MeV. Thus, if one takes the $\chi_{c2}(3P)$ as an assignment of the $X(4350)$, the precision measurements are needed in further experiments. The relative ratios

$\frac{\Gamma(\chi_{c2}(3P)\to D\bar{D})}{\Gamma(\chi_{c2}(3P)\to D^*\bar{D}^*)} \approx 0.30$ and $\frac{\Gamma(\chi_{c2}(3P)\to DD^*)}{\Gamma(\chi_{c2}(3P)\to D^*\bar{D}^*)} \approx 0.094$ with $M_{\chi_{c2}(3P)} = 4350.0$ MeV, also can provide evidence to discover the $X(4350)$ for the future experiment.

D. $h_c(2P)$ and $h_c(3P)$

Finally, we study the higher charmonium states with $J^{PC} = 1^{+-}$, $h_c(2P)$ and $h_c(3P)$. The $M_{h_c(2P)} = 3943.0$ MeV is consistent with the mass of the relativized Godfrey-Isgur model (3956 MeV) and the nonrelativistic potential model (3934 MeV) [26]. The $M_{h_c(3P)} = 4242.4$ MeV is close to the results of the nonrelativistic potential model (4279 MeV) [26]. And the two-body open charm strong decay results are shown in Table V. The $h_c(2P)$ has one decay mode $1^{+-} \to 0^-1^-$, and only can decay into DD^*. The total strong decay width $\Gamma_{h_c(2P)} = 48$ MeV, which is smaller than the results of other theoretical models.

The main decay modes of the $h_c(3P)$ include $1^{+-} \to 0^-1^-, 1^-1^-, 0^-0^+$. The final states DD^*, $D^*\bar{D}^*$, $D_sD_s^*$, $D_s^*D_s^*$, DD_0 are allowed. The total strong decay width $\Gamma_{h_c(3P)} = 31$ MeV is in accordance with the result of

TABLE V. The strong decay type and decay widths of the $h_c(2P)$ and $h_c(3P)$ (units in MeV).

Meson	State	Mode	Our result	LP(SP) [24]	[26]	[28]
h_c	2^1P_1	DD^*	48	64(68)	87	67
	3^1P_1	DD^*	16.0	14(11)	3.0	$\cdots$
		$D^*\bar{D}^*$	3.6	4.8(7.5)	22	$\cdots$
		$D_sD_s^*$	6.4	6.5(6.3)	15	$\cdots$
		$D_s^*D_s^*$	0.2	3.6(–)	7.5	$\cdots$
		DD_0	4.6	15(5.0)	28	$\cdots$
		Total	31	44(30)	75	$\cdots$

the screened potential quark model (30 MeV) [24]. The main decay channel $h_c(3P) \to DD^*$ contributes about 52% of the total strong decay width. The corresponding relative ratios: $\frac{\Gamma(h_c(3P) \to D^* \bar{D}^*)}{\Gamma(h_c(3P) \to DD^*)} \approx 0.23$ and $\frac{\Gamma(h_c(3P) \to D_s D_s^*)}{\Gamma(h_c(3P) \to DD^*)} \approx 0.40$ can provide theoretical assistance to confirm the $h_c(3P)$ in future experiments.

IV. SUMMARY

In conclusion, we have studied the two-body open charm strong decays of the $2P$ and $3P$ charmonium states by the BS method combined with the $^3P_0$ model. The wave functions and mass spectra of the initial $2P$ and $3P$ charmonium states are obtained by solving the BS equation with the relativistic correction. Considering the relativistic correction, the masses of some $3P$ charmonium states in our model will have a difference with the results of the nonrelativistic potential model. Then we get the two-body open charm strong decay widths of the $2P$ and $3P$ charmonium states.

Considering the $X^*(3860)$ as $\chi_{c0}(2P)$, the narrow strong decay width is smaller than the experimental data, because the strong decay width depend on the parameter, and there are large errors in the mass and the width of the $X^*(3860)$, we cannot rule out that the $X^*(3860)$ is $\chi_{c0}(2P)$. Taking the $X(4160)$ as the $\chi_{c0}(3P)$, the total strong decay width is in accordance with the experimental result of the $X(4160)$ with the uncertainty. In addition, because of the node structure of the $\chi_{c0}(3P)$'s wave functions, the integrand oscillates accordingly in the amplitude, the decay $X(4160) \to D\bar{D}$ is strong suppressed. Then the relative ratios $\frac{\Gamma(\chi_{c0}(3P) \to D\bar{D})}{\Gamma(\chi_{c0}(3P) \to D^* \bar{D}^*)} \approx 0.0019 < 0.09$, and $\frac{\Gamma(\chi_{c0}(3P) \to D\bar{D}^*)}{\Gamma(\chi_{c0}(3P) \to D^* \bar{D}^*)} = 0 < 0.22$ are consistent with the experimental results. Therefore, the $X(4160)$ is a good candidate for the $\chi_{c0}(3P)$.

Assigning the $X(4274)$ as the $\chi_{c1}(3P)$, we find that the total strong decay width is in agreement with the data of the $X(4274)$, so the $X(4274)$ resonance is a good candidate for the $\chi_{c1}(3P)$. The relative ratios $\frac{\Gamma(\chi_{c1}(3P) \to D^* \bar{D}^*)}{\Gamma(\chi_{c1}(3P) \to DD^*)} \approx 0.59$ and $\frac{\Gamma(\chi_{c1}(3P) \to D_s D_s^*)}{\Gamma(\chi_{c1}(3P) \to DD^*)} \approx 0.41$ can provide useful information in experiments.

The $Z(3930)$ has been confirmed as the $\chi_{c2}(2P)$ state in our previous work, so we only show the strong decay width in this work. Considering the $X(4350)$ as $\chi_{c2}(3P)$, we find that the total strong decay width of the $\chi_{c2}(3P)$ is larger than the result of the $X(4350)$, thus, if we take the $\chi_{c2}(3P)$ as an assignment of the $X(4350)$, we need many more investigations in the future.

Finally, we also calculate the two-body open charm strong decay of the $h_c(2P)$ and $h_c(3P)$, and give the total strong decay widths of the $h_c(2P)$ and $h_c(3P)$. The corresponding relative ratios $\frac{\Gamma(h_c(3P) \to D^* \bar{D}^*)}{\Gamma(h_c(3P) \to DD^*)} \approx 0.23$ and $\frac{\Gamma(h_c(3P) \to D_s D_s^*)}{\Gamma(h_c(3P) \to DD^*)} \approx 0.40$ can give the theoretical assistance in future experiments.

APPENDIX A: INSTANTANEOUS BETHE-SALPETER EQUATION

The BS equation which is used to describe the heavy mesons can be written as [58]

$$(\not{p}_1 - m_1)\chi(q)(\not{p}_2 + m_2) = i \int \frac{d^4 k}{(2\pi)^4} V(P, k, q)\chi(k), \quad \text{(A1)}$$

where $\chi(q)$ and P are the wave function and the momentum of the bound state, respectively. q is the relative momentum between quark and antiquark in the meson, $p_1 = \frac{m_1}{m_1 + m_2} P + q$, $p_2 = \frac{m_2}{m_1 + m_2} P - q$ and m_1, m_2 are the momentum and the mass of the quark and antiquark, respectively. The $V(P, k, q)$ is the interaction kernel between the quark and antiquark.

In order to solve Eq. (A1), the instantaneous approximation is adopted in the interaction kernel $V(P, k, q)$ [59]:

$$V(P, k, q) \Rightarrow V(|\vec{k} - \vec{q}|).$$

For convenience, the relative momentum q is decomposed into two parts $q_\parallel$ and $q_\perp$,

$$q^\mu = q_\parallel^\mu + q_\perp^\mu,$$
$$q_\parallel^\mu \equiv (q_P/M)P^\mu, \qquad q_\perp^\mu \equiv q^\mu - q_\parallel^\mu, \qquad q_P = P \cdot q/M.$$

Then Eq. (A1) can be expressed as

$$\chi(q_\parallel, q_\perp) = S_1(p_1)\eta(q_\perp)S_2(p_2). \quad \text{(A2)}$$

$\eta(q_\perp^\mu)$ is related to three-dimensional BS wave function $\varphi_P(q_\perp^\mu)$ as follows:

$$\varphi_P(q_\perp^\mu) \equiv i \int \frac{dq_p}{2\pi} \chi(q_\parallel^\mu, q_\perp^\mu),$$
$$\eta(q_\perp^\mu) \equiv \int \frac{dk_\perp}{(2\pi)^3} V(k_\perp, q_\perp)\varphi_p(k_\perp^\mu). \quad \text{(A3)}$$

$S_1(p_1)$ and $S_2(p_2)$ are the propagators of the quark and antiquark, which can be decomposed as

$$S_i(p_i) = \frac{\Lambda_{ip}^+(q_\perp)}{J(i)q_p + \alpha_i M - \omega_i + i\epsilon} + \frac{\Lambda_{ip}^-(q_\perp)}{J(i)q_p + \alpha_i M + \omega_i - i\epsilon}, \quad \text{(A4)}$$

with

$$\omega_i = \sqrt{m_i^2 + q_T^2},$$

$$\Lambda_{ip}^{\pm}(q_\perp) = \frac{1}{2\omega_{ip}}\left[\frac{\not{P}}{M}\omega_i \pm J(i)(m_i + \not{q}_\perp)\right], \quad \text{(A5)}$$

where $i = 1, 2$ for quark and antiquark, respectively, and $J(i) = (-1)^{i+1}$.

The positive and negative energy projected wave functions $\varphi_p^{\pm\pm}(q_\perp)$ are defined as

$$\varphi_p^{\pm\pm}(q_\perp) \equiv \Lambda_{1p}^{\pm}(q_\perp)\frac{\not{P}}{M}\varphi_p(q_\perp)\frac{\not{P}}{M}\Lambda_{2p}^{\pm}(q_\perp). \quad \text{(A6)}$$

Then under instantaneous approximation, with contour integration over q_p on both sides of Eq. (A2), we obtain the full Salpeter equation:

$$(M - \omega_1 - \omega_2)\varphi_p^{++}(q_\perp) = \Lambda_{1p}^{+}(q_\perp)\eta_p(q_\perp)\Lambda_{2p}^{+}(q_\perp),$$

$$(M + \omega_1 + \omega_2)\varphi_p^{--}(q_\perp) = -\Lambda_{1p}^{-}(q_\perp)\eta_p(q_\perp)\Lambda_{2p}^{-}(q_\perp),$$

$$\varphi_p^{+-}(q_\perp) = \varphi_p^{-+}(q_\perp) = 0. \quad \text{(A7)}$$

The wave functions are different for the bound states with different quantum J^{PC} (or J^P). First, we give the original BS wave functions for the different bound state, then reduce the wave functions through the last equation of Eq. (A7). Finally the numerical result of the wave functions and mass spectrum are obtained by solving the first and second equations in Eq. (A7). And the detailed solution of the Salpeter equation also has been discussed in Refs. [41,42,60,61].

To solve the Eq. (A7), we take the Cornell potential as the instantaneous interaction kernel V, which include a linear scalar interaction and a vector interaction. In the momentum space and the center of mass system of the bound state, the interaction potential is read as

$$V(\vec{q}) = V_s(\vec{q}) + \gamma_0 \otimes \gamma^0 V_v(\vec{q}),$$

$$V_s(\vec{q}) = -\left(\frac{\lambda}{\alpha} + V_0\right)\delta^3(\vec{q}) + \frac{\lambda}{\pi^2}\frac{1}{(\vec{q}^2 + \alpha^2)^2},$$

$$V_v(\vec{q}) = -\frac{2}{3\pi^2}\frac{\alpha_s(\vec{q})}{(\vec{q}^2 + \alpha^2)}, \quad \text{(A8)}$$

where λ is the string constant and $\alpha_s(\vec{q}) = \frac{12\pi}{33-2N_f}$ $\frac{1}{\log(a+\vec{q}^2/\Lambda_{\text{QCD}}^2)}$ is the running coupling constant. In order to fit the data of heavy quarkonia, a constant V_0 is often added to confining potential. We also introduce a small parameter a to avoid the divergence in the denominator. The constants λ, α, V_0, and Λ_{QCD} are the parameters that characterize the potential.

APPENDIX B: THE RELATIVISTIC WAVE FUNCTIONS

In this paper, we focus on the OZI-allowed two-body open charm strong decay of the $2P$ and $3P$ charmonium states. The detailed wave functions have been obtained in Refs. [41,42,60,61]. We mainly introduce the relativistic BS wave functions of the χ_{c0}, χ_{c1}, χ_{c2}, and h_c in this section.

1. The relativistic BS wave function of the χ_{c0} with $J^{PC} = 0^{++}$

The original BS wave functions of the χ_{c0} with $J^{PC} = 0^{++}$ can be written as

$$\varphi_{0^{++}}(q_\perp) = M\left[\frac{\not{q}_\perp}{M}f_1(q_\perp) + \frac{\not{P}\not{q}_\perp}{M^2}f_2(q_\perp) + f_3(q_\perp)\right.$$
$$\left. + \frac{\not{P}}{M}f_4(q_\perp)\right], \quad \text{(B1)}$$

where M is the mass of bound state χ_{c0}, $f_i(q_\perp)$ is the original radial wave functions that are related to $|\vec{q}|^2$. Taking Eq. (B1) to Eq. (A7), the relativistic BS wave functions and the mass spectrum can be obtained by solving the Salpeter equations (A7). Then the relativistic positive BS wave function is shown as

$$\varphi_{0^{++}}^{++}(q_\perp) = A_1(q_\perp) + \frac{\not{P}}{M}A_2(q_\perp) + \frac{\not{q}_\perp}{M}A_3(q_\perp)$$
$$+ \frac{\not{P}\not{q}_\perp}{M^2}A_4(q_\perp). \quad \text{(B2)}$$

The corresponding coefficients are

$$A_1 = \frac{(\omega_1 + \omega_2)q_\perp^2}{2(m_1\omega_2 + m_2\omega_1)}\left[f_1 + \frac{m_1 + m_2}{\omega_1 + \omega_2}f_2\right],$$

$$A_2 = \frac{(m_1 - m_2)q_\perp^2}{2(m_1\omega_2 + m_2\omega_1)}\left[f_1 + \frac{m_1 + m_2}{\omega_1 + \omega_2}f_2\right],$$

$$A_3 = \frac{M}{2}\left[f_1 + \frac{m_1 + m_2}{\omega_1 + \omega_2}f_2\right], \quad A_4 = \frac{M}{2}\left[\frac{\omega_1 + \omega_2}{m_1 + m_2}f_1 + f_2\right],$$

where m_1, m_2 and $\omega_1 = \sqrt{m_1^2 + \vec{q}^2}$, $\omega_2 = \sqrt{m_2^2 + \vec{q}^2}$ are the masses and the energies of the quark and antiquark in the χ_{c0} state.

2. The relativistic BS wave function of the χ_{c1} with $J^{PC} = 1^{++}$

The original BS wave functions of the χ_{c1} with $J^{PC} = 1^{++}$ is constructed by P, $q_\perp$, and the polarization vector ϵ,

$$\varphi_{1^{++}}(q_\perp) = i\varepsilon_{\mu\nu\alpha\beta}\frac{P^\nu}{M}q_\perp^\alpha \epsilon^\beta \left[g_1\gamma^\mu + g_2\frac{\not P}{M}\gamma^\mu + g_3\frac{\not q_\perp}{M}\gamma^\mu + g_4\frac{\not P\gamma^\mu \not q_\perp}{M^2}\right], \tag{B3}$$

where ϵ is the polarization vector of the axial vector meson. The corresponding relativistic positive BS wave function is obtained in Eq. (B4) by solving Eq. (A7),

$$\varphi_{1^{++}}^{++}(q_\perp) = i\varepsilon_{\mu\nu\alpha\beta}\frac{P^\nu}{M}q_\perp^\alpha \epsilon^\beta \gamma^\mu \left[B_1 + B_2\frac{\not P}{M} + B_3\frac{\not q_\perp}{M} + B_4\frac{\not P\not q_\perp}{M^2}\right], \qquad B_1 = \frac{1}{2}\left[g_1 + \frac{\omega_1 + \omega_2}{m_1 + m_2}g_2\right],$$

$$B_2 = -\frac{1}{2}\left[\frac{m_1 + m_2}{\omega_1 + \omega_2}g_1 + g_2\right], \qquad B_3 = \frac{M(\omega_1 - \omega_2)}{m_1\omega_2 + m_2\omega_1}B_1, \qquad B_4 = -\frac{M(m_1 + m_2)}{m_1\omega_2 + m_2\omega_1}B_1. \tag{B4}$$

3. The relativistic BS wave function of the χ_{c2} with $J^{PC} = 2^{++}$

The original BS wave function of the χ_{c2} is constructed by P, $q_\perp$, the polarization tensor $\epsilon_{\mu\nu}$ and the gamma matrices,

$$\varphi_{2^{++}}(q_\perp) = \epsilon_{\mu\nu}q_\perp^\mu q_\perp^\nu \left[h_1(q_\perp) + \frac{\not P}{M}h_2(q_\perp) + \frac{\not q_\perp}{M}h_3(q_\perp) + \frac{\not P\not q_\perp}{M^2}h_4(q_\perp)\right]$$

$$+ M\epsilon_{\mu\nu}\gamma^\mu q_\perp^\nu \left[h_5(q_\perp) + \frac{\not P}{M}h_6(q_\perp) + \frac{\not q_\perp}{M}h_7(q_\perp) + \frac{\not P\not q_\perp}{M^2}h_8(q_\perp)\right], \tag{B5}$$

where $\epsilon_{\mu\nu}$ is the polarization tensor of the χ_{c2} with $J^{PC} = 2^{++}$. According to the solution of Eq. (A7), we get the relativistic positive BS wave function,

$$\varphi_{2^+}(q_\perp) = \epsilon_{\mu\nu}q_\perp^\mu q_\perp^\nu \left[C_1(q_\perp) + \frac{\not P}{M}C_2(q_\perp) + \frac{\not q_\perp}{M}C_3(q_\perp) + \frac{\not P\not q_\perp}{M^2}C_4(q_\perp)\right]$$

$$+ M\epsilon_{\mu\nu}\gamma^\mu q_\perp^\nu \left[C_5(q_\perp) + \frac{\not P}{M}C_6(q_\perp) + \frac{\not q_\perp}{M}C_7(q_\perp) + \frac{\not P\not q_\perp}{M^2}C_8(q_\perp)\right], \tag{B6}$$

where the coefficients are

$$C_1 = \frac{1}{2M(m_1\omega_2 + m_2\omega_1)}[(\omega_1 + \omega_2)q_\perp^2 h_3 + (m_1 + m_2)q_\perp^2 h_4 + 2M^2\omega_2 h_5 - 2M^2 m_2 h_6],$$

$$C_2 = \frac{1}{2M(m_1\omega_2 + m_2\omega_1)}[(m_1 - m_2)q_\perp^2 h_3 + (\omega_1 - \omega_2)q_\perp^2 h_4 - 2M^2 m_2 h_5 + 2M^2\omega_2 f_6],$$

$$C_3 = \frac{1}{2}\left[h_3 + \frac{m_1 + m_2}{\omega_1 + \omega_2}h_4 - \frac{2M^2}{m_1\omega_2 + m_2\omega_1}h_6\right], \qquad C_4 = \frac{1}{2}\left[\frac{\omega_1 + \omega_2}{m_1 + m_2}h_3 + h_4 - \frac{2M^2}{m_1\omega_2 + m_2\omega_1}h_5\right],$$

$$C_5 = \frac{1}{2}\left[h_5 - \frac{\omega_1 + \omega_2}{m_1 + m_2}h_6\right], \qquad C_6 = \frac{1}{2}\left[-\frac{m_1 + m_2}{\omega_1 + \omega_2}h_5 + h_6\right],$$

$$C_7 = \frac{M}{2}\frac{\omega_1 - \omega_2}{m_1\omega_2 + m_2\omega_1}\left[h_5 - \frac{\omega_1 + \omega_2}{m_1 + m_2}h_6\right], \qquad C_8 = \frac{M}{2}\frac{m_1 + m_2}{m_1\omega_2 + m_2\omega_1}\left[-h_5 + \frac{\omega_1 + \omega_2}{m_1 + m_2}h_6\right].$$

4. The relativistic BS wave function of the h_c with $J^{PC} = 1^{+-}$

The original BS wave functions of the h_c with $J^{PC} = 1^{+-}$ also is constructed by P, $q_\perp$ and the polarization vector ϵ,

$$\varphi_{1^{+-}}(q_\perp) = q_\perp \cdot \epsilon \left[t_1(q_\perp) + \frac{\not P}{M}t_2(q_\perp) + \frac{\not q_\perp}{M}t_3(q_\perp) + \frac{\not P\not q_\perp}{M^2}t_4(q_\perp)\right]\gamma_5, \tag{B7}$$

where ϵ is the polarization vector of the h_c. The corresponding relativistic positive BS wave function is obtained in Eq. (B4) by solving Eq. (A7),

$$\varphi_{1^{+-}}^{++}(q_\perp) = q_\perp \cdot \epsilon \left[K_1(q_\perp) + \frac{\slashed{P}}{M} K_2(q_\perp) + \frac{\slashed{q}_\perp}{M} K_3(q_\perp) + \frac{\slashed{P}\slashed{q}_\perp}{M^2} K_4(q_\perp) \right] \gamma_5, \tag{B8}$$

where the coefficients are

$$K_1 = \frac{1}{2} \left[t_1 + \frac{\omega_1 + \omega_2}{m_1 + m_2} t_2 \right], \qquad K_2 = \frac{1}{2} \left[\frac{m_1 + m_2}{\omega_1 + \omega_2} t_1 + t_2 \right],$$

$$K_3 = -\frac{M(\omega_1 - \omega_2)}{m_1\omega_2 + m_2\omega_1} K_1, \qquad K_4 = -\frac{M(m_1 + m_2)}{m_1\omega_2 + m_2\omega_1} K_1.$$

[1] S. K. Choi *et al.* (Belle Collaboration), Phys. Rev. Lett. **91**, 262001 (2003).

[2] P. Pakhlov *et al.* (Belle Collaboration), Phys. Rev. Lett. **100**, 202001 (2008).

[3] T. Aaltonen *et al.* (CDF Collaboration), Phys. Rev. Lett. **102**, 242002 (2009).

[4] T. Aaltonen *et al.* (CDF Collaboration), Mod. Phys. Lett. A **32**, 1750139 (2017).

[5] R. Aaij *et al.* (LHCb Collaboration), Phys. Rev. Lett. **118**, 022003 (2017).

[6] R. Aaij *et al.* (LHCb Collaboration), Phys. Rev. D **95**, 012002 (2017).

[7] M. Tanabashi *et al.* (Particle Data Group), Phys. Rev. D **98**, 030001 (2018).

[8] B. Aubert *et al.* (*BABAR* Collaboration), Phys. Rev. D **81**, 092003 (2010).

[9] X. Liu, Chin. Sci. Bull. **59**, 3815 (2014).

[10] H. X. Chen, W. Chen, X. Liu, and S. L. Zhu, Phys. Rep. **639**, 1 (2016).

[11] C. P. Shen *et al.* (Belle Collaboration), Phys. Rev. Lett. **104**, 112004 (2010).

[12] K. Chilikin *et al.* (Belle Collaboration), Phys. Rev. D **95**, 112003 (2017).

[13] D. Y. Chen, Eur. Phys. J. C **76**, 671 (2016).

[14] H. X. Chen, E. L. Cui, W. Chen, X. Liu, and S. L. Zhu, Eur. Phys. J. C **77**, 160 (2017).

[15] W. Chen and S. L. Zhu, Phys. Rev. D **83**, 034010 (2011).

[16] J. Ferretti, E. Santopinto, M. Naeem Anwar, and Y Lu, Eur. Phys. J. C **80**, 464 (2020).

[17] H. F. Fu and L. B. Jiang, Eur. Phys. J. C **79**, 460 (2019).

[18] M. X. Duan, S. Q. Luo, X. Liu, and T. Matsuki, Phys. Rev. D **101**, 054029 (2020).

[19] D. Y. Chen, X. Liu, and T. Matsuki, Prog. Theor. Exp. Phys. **2015**, 43B05 (2015).

[20] B. L. Huang, Z. Y. Lin, and S. L. Zhu, Phys. Rev. D **105**, 036016 (2022).

[21] C. R. Deng, H. Chen, and J. L. Ping, Phys. Rev. D **103**, 014001 (2021).

[22] W. Hao, G. Y. Wang, E. Wang, G. N. Li, and D. M. Li, Eur. Phys. J. C **80**, 626 (2020).

[23] X. Liu, Z. G. Luo, and Z. F. Sun, Phys. Rev. Lett. **104**, 122001 (2010).

[24] L. C. Gui, L. S. Lu, Q. F. Lu, X. H. Zhong, and Q. Zhao, Phys. Rev. D **98**, 016010 (2018).

[25] W. Chen, H. X. Chen, X. Liu, T. G. Steele, and S. L. Zhu, Phys. Rev. D **96**, 114017 (2017).

[26] T. Barnes, S. Godfrey, and E. S. Swanson, Phys. Rev. D **72**, 054026 (2005).

[27] M. X. Duan and X. Liu, Phys. Rev. D **104**, 074010 (2021).

[28] E. S. Swanson, Phys. Rep. **429**, 243 (2006).

[29] B. Q. Li and K. T. Chao, Phys. Rev. D **79**, 094004 (2009).

[30] T. Branz, R. Molina, and E. Oset, Phys. Rev. D **83**, 114015 (2011).

[31] V. Kher and A. K. Rai, Chin. Phys. C **42**, 083101 (2018).

[32] Z. H. Wang, Y. Zhang, T. H. Wang, Y. Jiang, and G. L. Wang, Eur. Phys. J. C **80**, 791 (2020).

[33] Z. H. Wang, Y. Zhang, L. B. Jiang, T. H. Wang, Y. Jiang, and G. L. Wang, Eur. Phys. J. C **77**, 43 (2017).

[34] T. H. Wang and G. L. Wang, Phys. Lett. B **697**, 233 (2011).

[35] T. H. Wang, G. L. Wang, Y. Jiang, and W. L. Ju, J. Phys. G **40**, 035003 (2013).

[36] T. H. Wang, G. L. Wang, H. F. Fu, and W. L. Ju, J. High Energy Phys. 07 (2013) 120.

[37] L. Micu, Nucl. Phys. **B10**, 521 (1969).

[38] Z. F. Sun and X. Liu, Phys. Rev. D **80**, 074037 (2009).

[39] J. Segovia, D. R. Entem, and F. Fernández, Phys. Lett. D **715**, 322 (2012).

[40] H. F. Fu, X. J. Chen, G. L. Wang, and T. H. Wang, Int. J. Mod. Phys. A **27**, 1250027 (2012).

[41] C. S. Kim and G. L. Wang, Phys. Lett. B **584**, 285 (2004).

[42] C. H. Chang and G. L. Wang, Sci. China Series G, **53**, 2005 (2010).

[43] F. K. Guo and U. G. Meißner, Phys. Rev. D **86**, 091501 (2012).

[44] G. L. Yu, Z. G. Wang, and Z. Y. Li, Chin. Phys. C **42**, 043107 (2018).

[45] K. T. Chao, Phys. Lett. B **661**, 348 (2008).

[46] H. Wang, Z. Z. Yan, and J. L. Ping, Eur. Phys. J. C **75**, 196 (2015).

[47] Y. C. Yang, Z. R. Xia, and J. L. Ping, Phys. Rev. D **81**, 094003 (2010).

[48] T. Barnes and S. Godfrey, Phys. Rev. D **69**, 054008 (2004).

[49] E. J. Eichten, K. Lane, and C. Quigg, Phys. Rev. D **69**, 094019 (2004).

[50] M. Suzuki, Phys. Rev. D **72**, 114013 (2005).

[51] S. L. Olsen, Front. Phys. China. **10**, 121 (2015).

[52] F. K. Guo, C. Hanhart, U. G. Meißner, Q. Wang, Q. Zhao, and B. S. Zou, Rev. Mod. Phys. **90,** 015004 (2018).

[53] R. F. Lebed, R. E. Mitchell, and E. S. Swanson, Prog. Part. Nucl. Phys. **93,** 143 (2017).

[54] J. Ferretti, G. Galatá, and E. Santopinto, Phys. Rev. D **90,** 054010 (2014).

[55] L. Meng, G. J. Wang, B. Wang, and S. L. Zhu, Phys. Rev. D **104,** 094003 (2021).

[56] H. Wang, Y. C. Yang, and J. L. Ping, Eur. Phys. J. A **50,** 76 (2014).

[57] P. G. Ortega, J. Segovia, D. R. Entem, and F. Fernández, Phys. Lett. B **778,** 1 (2018).

[58] E. E. Salpeter and H. A. Bethe, Phys. Rev, **84,** 1232 (1951).

[59] E. E. Salpeter, Phys. Rev, **87,** 328 (1952).

[60] C. H. Chang, J. K. Chen, and G. L. Wang, Commun. Theor. Phys. **46,** 467 (2006).

[61] G. L. Wang, Phys. Lett. B **650,** 15 (2007).